Journal of Engineering and Applied Sciences 13 (24): 10502-10509, 2018
ISSN: 1816-949X

Prediction of Cutting Tool Performance with Double Rake Geometry Using Finite Element Technique

[1]Saad T. Faris, [2]Salem F. Salman and [2]Muzher T. Mohamed
[1]Department of Mechanical Engineering,
[2]Department of Material Engineering, University of Diyala, 32001 Baqubah, Iraq

Abstract: This research deals with the determination of cutting performance of the Iraqi carbide tools with double rake geometry with negative/positive combination through the stress distribution within and at the boundaries of the tool wedge. A modification in geometry was achieved using the finite element technique by considering the cutting tool in a plane strain employing the MSC/Nastran package. An experimental work was also conducted on double rake geometry produced by grinding a negative land on the rake face. The double rake geometry was varied in primary rake angle (-10, -20 and -40°) and the land width of (0.1, 0.3, 0.5 and 0.8) of the initial carbide using optimum geometry obtained from stress analysis. The result demonstrate that at negative and positive rake geometry and at the point of zero stresses the type of stress changes from compression to tension and they are shifted away on the cutting edge leaving more space on the top of the rake cutting zone under compression.

Key words: Modeling, cutting tool, FEM, double rake geometry, stresses, primary rake

INTRODUCTION

Cutting edge geometry modifications have been investigated by many researchers. Chao and Trigger reported the results of an investigation on the performance of controlled as restricted contact cutting tools. They found that there is a substantial reduction in power consumption on increase in tool life, more effective utilization of cutting fluids on improved surface finish and the cutting forces were also found to be lower with restricted tools. Bagley (1961) investigated the double rake geometries using a ceramic cutting tool material. The tool had a negative primary rake of 45° with land width being varied up to a value of 1.65 mm. Hardened tool steels (62Rc) were turned with a feed rate of 0.127 mm/rev and a speed of 123 m/min. It was found that the addition negative land strengthened the cutting edge and reduced the initial breakdown giving improved tool life compared with positive rake tool. Zorev (1963) found that an optimum land width to the feed ratio of 1.55 was found when machining steel at different levels of tensile strength and feed rate. The formula for optimum land width found in relation to both cutting speed and feed rate was:

$$\text{Optimum width} = \frac{f^{0.45}}{V^{0.23}}$$

Draper (1974) and Barrow (1977) investigated the cutting performance of double rake angle tools. A negative land was ground on to positive rake cutting tool to simulate the change in shape due to the deformation at the cutting edge. It was concluded that there is no fixed relationship between the feed and land width as was claimed by previous researchers. The land width used is established by machining experiments. Fowler (1980) achieved double rake work on both carbide and coated carbide tool materials. It was found that significant improvement was achieved in the cutting performance, partially with regard to catastrophic failure when cutting steel was achieved depending upon the cutting conditions. Chandrasekaran and Nagarajan (1977) studied the stress distribution on tool using photoelastic method. A comprehensive model for the distribution of contact stresses along the wear land is proposed and an experimental result obtained from photoelastic investigation of lead was carried out at low speed and contact depth of cut, making use of transparent epoxy tool provided with a pre-honed wear flat along the flank surface.

Ahmed *et al.* (1989) made a study on the prediction of cutting tool performance by using FEM. The researcher described an analysis of cutting tool performance through a determination of the stress distribution within and at the boundaries was based on a two dimensional model, using a range of cutting geometries including tools with double rake angles. Younis (1992) made a study on mechanical and thermal stresses in clamped, brazed and bonded carbides. A model based on the FEM is presented for determining thermal and mechanical stresses in the carbide insert due to heat and cutting forces induced

Corresponding Author: Salem F. Salman, Department of Material Engineering, University of Diyala, 32001 Baqubah, Iraq

during metal cutting. In this they found a model of loading at tool tip. The normal stress on the rake face is a maximum at the tool end of the contact length.

Thus, there is a lack in information about this field. In these days, cutting tool inserts are manufactured and used by many industrial companies with high rate of production, so, the proper design of these inserts will help these factories to reduce costs of machining. In order to achieve this a stress analysis to the carbide inserts. Many types of test are conduct on metal specimen in order to ascertain their different mechanical properties, determine the surface of subsurface defect, check chemical composion and thus their suitability for specific uses, the data obtained from these is conforms to the required specification or not. This helps in the selection of suitable material for a specitic use and also its soundness (Wadhwa, 2012).

MATERIALS AND METHODS

Theory: The cutting process is a complex phenomenon and involves different processes which take place at the same time during machining. The machining variables are cutting speed, feed and depth of cut and rigidity of the machine. The cutting speed is influenced strongly by the geometric elements, i.e., (the plane approach angle), the larger angle, the larger the uncut chip thickness and the shorter the active section of the cutting edge.

The rate of feed and depth of cut depend upon many variables such as the rigidity of tool and work piece material. In turning, there is a relationship between cutting speed, feed and depth of cut for a specific tool life. The machine tool should be sufficiently rigid. This means that spindle bearing should be adequate and well fitted. All sliding parts need to be adjusted. Stress concentration factor high localized stresses created by an abrupt change of form discontinuity occurs in such frequently encountered configuration as hole, notch and fillets. The formulas in some cases the stress and accompanying formation near a discontinuity can be analyzed by applying the theory of elasticity (Vgural, 2009).

Stresses in metal cutting process: One of the most important aspects of the chip formation process is the nature of the mean compressive and shear stress acting on the tool and the way that they are distributed along the rake face. The most of the failure modes in machine design originate high loads, a stress analysis is almost invariably needed for every machine design analysis. The study of stresses and strain at the chip formation zone is useful in explaining the mechanics and thermal aspects of machining in terms of the physical parameters (Yield strength, Strain hardening level, ..., etc.). The tool may undergo brittle or plastic failure. Such failure can be analyzed with the knowledge of the cutting tool stresses (Beer *et al*., 2014). Different types of stresses developed in cutting process.

Non-cutting stresses: Which are the residual stresses due to manufacturing process, brazing stresses resulted from the preparation of the brazed tool to suit correct geometrical requirement and the cutting stresses which are induced from cutting force which acts along the cutting edges and from the temperature such as the contact stresses which are produced on the contact chip length which are normal and shear stresses.

Cutting stress: These type of stresses come from the cutting force which acts along the cutting edges and from the temperature which has an elevated value during cutting. This type of stress is affected by cutting parameters like (cutting speed, depth of cut, feed) and tool geometry parameters like (tool angles, type of rake angle, etc.).

Thermal stresses: This type of stress is produced by temperature gradient which occurs in the cutting edge during cutting. During cutting the combination between thermal and mechanical loading is very important because most tools fail before they reach yield stresses due to working at high temperature which is produced by friction between tool and work piece (Venkatesh and Chandrasekaran, 1982).

Calculation of cutting stresses: The cutting tool fail in a brittle manner due to lack of strength. Figure 1 shows the bending of the wedge-shaped tool subjected to a distributed load within the region of contact length C. the

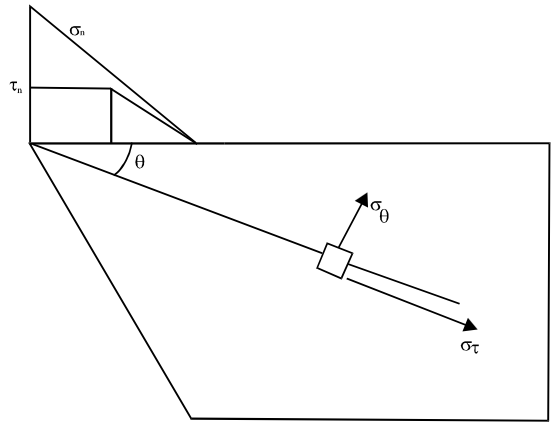

Fig. 1: Stress components in a cutting tool

generated stresses in the tool up to the contact length expressed in polar coordinates r and θ are (Sen and Bhattacharyya, 1999):

$$\sigma_r = 2(b_o+d_o-a_2\cos 2\theta-C_2\sin 2\theta)-r^n\{(n^2-n-2)(b_n\cos n\theta+ d_n\sin n\theta)(n+1)(n+2)[a_{n+2}\cos(n+2)\theta+C_n 2\sin(n+2)\theta]\} \quad (1)$$

$$\sigma_\theta = 2(b_o+d_o-a_2\cos 2\theta-C_2\sin 2\theta)+r^n(n+1)(n+ 2)[b_n\cos n\theta+d_n\sin n\theta+a_{n+2}\cos(n+2)\theta+ C_n\sin(n+2)\theta]+a_{n+2}\cos(n+2)\theta+C_n\sin(n+2)\theta\} \quad (2)$$

$$\tau_{r\theta} = 2(-0.5d_o+a_2\sin 2\theta-C_2\cos 2\theta)+r^n(n+ 1)\{n[b_n\sin n\theta-d_n\cos n\theta]+(n+2)[a_{n+2}\sin(n+ 2)\theta-C_n\cos(9n+2)\theta] \quad (3)$$

where, b_o, d_o, a_2, C_2, b_n, d_n, a_{n+2}, C_{n+2} are coefficients to be determined from the boundary conditions of the contact stress distribution and n is the index of the parabolic distributions. The boundary conditions are:

$$\sigma_\theta = -\sigma_n, \quad \text{at} \quad \theta = \alpha_o$$
$$\sigma_\theta = 0, \quad \text{at} \quad \theta = o+\beta$$
$$\tau_{r\theta} = -\tau_i, \quad \text{at} \quad \theta = \alpha_o$$
$$\tau_{r\theta} = 0, \quad \text{at} \quad \theta = o+\beta$$

Where:

α_o = The initial rake angle
β = The lip angle
σ_θ, σ_r, $\tau_{r\theta}$ = The values of σ_1, σ_2 can be calculated in the contact zone (0<r<c)

where, c is the length of natural contact. However, where r>>c, St. Venant's principle is applicable and the stresses may be calculated for concentrated loads shown in Fig. 2 and the stresses are given by:

$$\sigma_r = -\frac{2R}{rb}\left[\frac{\cos(\Delta-(\frac{\beta}{2}+\alpha_o))\cos(\theta-(\frac{\beta}{2}+\alpha_o))}{\beta+\sin\beta}+ \frac{\sin(\Delta-(\frac{\beta}{2}+\alpha_o))\sin(\theta-(\frac{\beta}{2}+\alpha_o))}{\beta+\sin\beta}\right. \quad (4)$$

Where:

b = Width of cut
σ_θ = 0
$\tau_{r\theta}$ = 0

The angle Δ is the direction of applied force R and is obtained from:

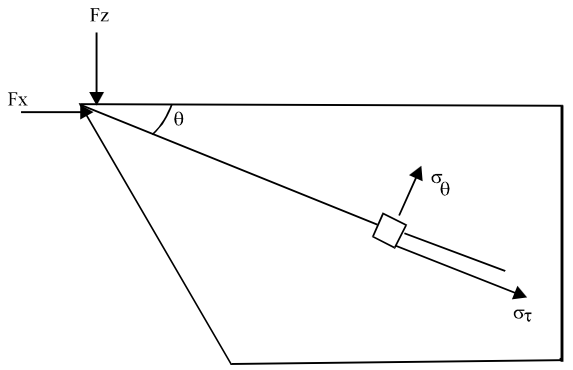

Fig. 2: Stress components and the complex length in cutting tool

$$\Delta = \tan^{-1}\left[\frac{F_z}{F_{xy}}\right] \quad (5)$$
$$R = \sqrt{F_z^2+F_{xy}^2}$$

Finite element modeling: The cutting tool is analyzed using the finite element technique by considering the tool in a plane strain condition with the following displacement fields:

$$u(\zeta,\eta) = N_1u_1+N_2u_2+N_3u_3+N_4u_4 \quad (6)$$
$$\upsilon(\zeta,\eta) = N_1\upsilon_1+N_2\upsilon_2+N_3\upsilon_3+N_4\upsilon_4$$

Where:

u and υ = The displacement components
x and y = Directions
N_i = The shape functions

The Cartesian coordinate system (x, y) and the intrinsic system (ζ, η) can be obtained by employing the isoperimetric formulation.

$$x(\zeta,\eta) = \sum_{i=0}^{4} x_iN_i(\zeta,\eta) \quad (7)$$
$$y(\zeta,\eta) = \sum_{i=0}^{4} y_iN_i(\zeta,\eta)$$

The Quad 4 was chosen as a discretization element. The strain tensor is given by:

$$\{\varepsilon\}^t = \{\varepsilon_x\ \varepsilon_y\ \gamma_{xy}\}^t \quad (8)$$

And the element stiffness matrix is given by:

$$[K]^e = \iiint_v [B]^t[D][B]dxdydz \quad (9)$$

where, [B] is the strain displacement relationship:

$$[B] = \begin{bmatrix} \frac{\partial N_i}{\partial x} & 0 & 0 \\ 0 & \frac{\partial N_i}{\partial y} & 0 \\ 0 & 0 & \frac{\partial N_i}{\partial z} \\ \frac{\partial N_i}{\partial y} & \frac{\partial N_i}{\partial x} & 0 \\ 0 & \frac{\partial N_i}{\partial z} & \frac{\partial N_i}{\partial y} \\ \frac{\partial N_i}{\partial z} & 0 & \frac{\partial N_i}{\partial x} \end{bmatrix} \quad (10)$$

And [D] is the elasticity matrix and is given by:

$$[D] = \frac{E}{(1+\upsilon)(1-2\upsilon)} \begin{bmatrix} 1-\upsilon & \upsilon & \upsilon & 0 & 0 & 0 \\ \upsilon & 1-\upsilon & \upsilon & 0 & 0 & 0 \\ \upsilon & \upsilon & 1-\upsilon & 0 & 0 & 0 \\ 0 & 0 & 0 & \frac{1-2\upsilon}{2} & 0 & 0 \\ 0 & 0 & 0 & 0 & \frac{1-2\upsilon}{2} & 0 \\ 0 & 0 & 0 & 0 & 0 & \frac{1-2\upsilon}{2} \end{bmatrix} \quad (11)$$

Formulation of the load vector: Using the data obtained from cutting test using dynamometer, the loads on the cutting tool are estimated. The load is taken as: distributed normal load varying from maximum value at the first point of contact between the tool and the workpiece and is linearly decreased until it reaches zero when the chip leaves the chip tool contact.

Distributed shear load which consists of two regions, the first one is a uniform distributed load which reaches till the mid point of the chip tool contact with cold sliding regions and the second one is sticking regions in which the load is decreased until it reaches zero when the chip leaves the chip tool contact. However, the typical finite element mesh is shown in Fig. 3.

Experimental programme: The experimental program carried out in University of Technology/Workshop Department/Automobile workshops. The machine used in performing the experimental work was universal testing machine. The centre lathe (Model SN 50B) manufactured by Tos Trenic Fig. 4 and 5. The range of speed is between (22.4-2000 rpm) while the maximum work diameter can be (250 mm). The chemical composition and the mean hardness, of the work piece material is given below, we use a valve facing equipment in the laboratory which used to modify the shape of valves to produce the double rake geometry.

Fig. 3: Mesh used in FEM and end of fixation

Fig. 4: Lathe machine used in experimental work

Fig. 5: Iraqi carbide insert used in experimental work

The initial tests on commercially available tools 12.7 mm square and 4.76 thick with 1.2 mm nose radius. The second set of experiment was made on modified insert which gives a double rake negative/positive combination with a land width of 0.5 mm and angle of (-25°). The experiments are divided into two groups: standard cutting tool: speed (50, 150 and 250 m/min), feed rate (0.16, 0.24, 0.4 and 0.56 mm) and depth of cut (0.5 mm).

Standard cutting tool with tool modification in geometry due to grinding a small portion to produced double rake with primary angle of 25° and land width of 0.25 mm. the same design variable mentioned in 1 are repeated here.

RESULTS AND DISCUSSION

The evaluation of the double rake cutting geometry is discussed here, Fig. 6 and 7 show the results of computed average stresses of cutting data for primary rake angle -10° for different land width (0.1, 0.3, 0.5 and 0.8 mm

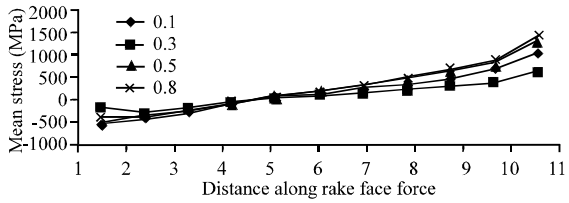

Fig. 6: Distribution of mean stress along rake face (primary angel -10, feed = 0.17 mm)

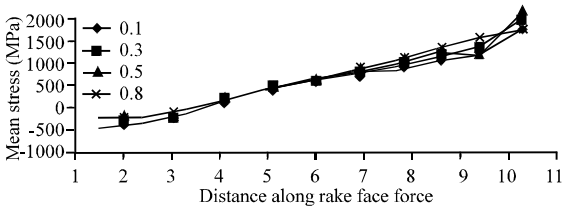

Fig. 7: Distribution of mean stress along rake face (primary angel -10, feed = 0.24 mm)

and for two values of feed rake). The same variables were presented for the primary rake angle -25° shown in Fig. 8-11 for the primary rake angle -40° keeping the secondary rake angle constant for all above cutting geometries.

The figures reveal similar trends, since, the average stresses appear to have a high compression value at the beginning of the cutting edge and begin to decrease towards the end of contact length between chip and rake face, the stress starts to decrease until it is converted to a tensile stress and increases to high value at the point of fixation of carbide insert as it fixed on the tool holder. For rake angle -10° for feed 0.16 mm/rev, the tip tool stress (-554 MPa) and starts to decrease until it reaches zero and as it moves away from the cutting edge it is converted to a tensile and increases to reach a value of (1017 MPa) at the point of fixation of the carbide inserts. Figure 6 and 7 show the distribution of mean stresses along the rake face the average stress (-500 MPa). As the primary rake angle is altered to -25° as shown in Fig. 8, the average stresses (feed 0.16 mm/rev, land width 0.1mm) is -553 MPa in compression at the tip and maximum tensile stress of (1131 MPa) at the same prescribed point changing the land width to 0.5 mm, the average stress becomes 400 MPa compression at the tip and maximum tensile stress at the tool fixation of (1217 MPa).

Increasing land width above 0.5 mm the average stress becomes (935 MPa) a compression at the tip and (1283 MPa) at the fixation point. However, the distribution of mean stresses for feed rate 0.24 is shown in Fig. 9. Figure 10 and 11 show the distribution of mean stresses

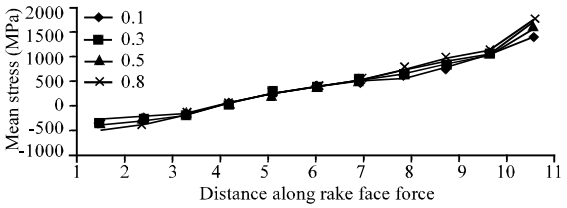

Fig. 8: Distribution of mean stress along rake face (primary angel -25, feed = 0.17 mm)

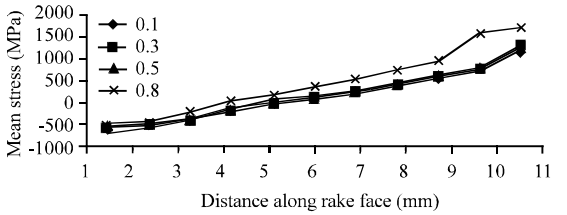

Fig. 9: Distribution of mean stress along rake face (primary angel -25, feed = 0.17 mm)

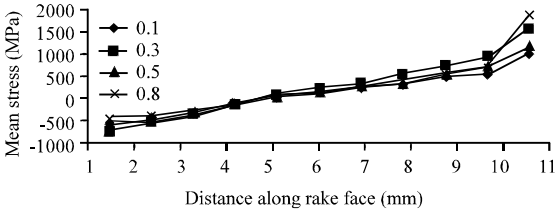

Fig. 10: Distribution of mean stress along rake face (primary angel -40, feed = 0.17 mm)

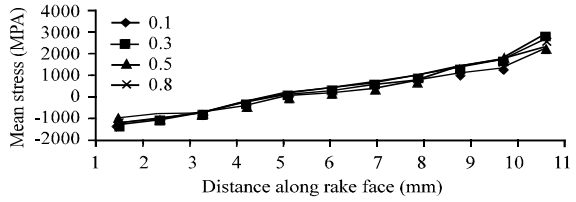

Fig. 11: Distribution of mean stress along rake face (primary angel -40, feed = 0.24 mm)

for the rake angle (-40°). To have an idea the distribution of mean stresses along the rake face, the computed average stresses are shown in Table 1-3 for primary rake angle -10° for different land width (0.1, 0.3, 0.5 and 0.8 mm). Results of other rake angle -250 and -40° are listed in Table 4-7, respectively. However, the maximum shear stress distribution is summarized in Table 8. This is an indication of failure of the tool according to this criterion and to obtain a fairly accurate correlation with the experimental results which attract the researches for the assessment of tool performance when the finite element is applied in cutting action studies (Table 9).

Table 1: Chemical composition and the mean hardness, of the work piece material

Varriables	Values
Mat	Ck-40
C	0.421
Si	0.281
Mn	0.83
Ni	-
P	0.023
S	0.014
Mo	0.04
Cr	0.115
Cu	-
V	0.003
Hr	144-145

Table 2: Results of mean stress, von Mises and τ max

Landwidth (mm)/0.1	0.3	0.5	0.8
Position along rake face			
-554	-202	-490	-436
-471	-308	-429	-381
-340	-187	-342	-328
-109	-45	-144	-141
51	28	47	58
131	77	154	177
229	134	284	319
310	202	434	482
450	284	614	676
664	370	775	848
1017	594	1294	1409

Table 3: Distribution of mean stress (MPa) along rake face for primary rake angle -10° and feed rate = 0.17mm/rev

Land width	Mean stress (MPa)	Von mises (MPa)	τ max (MPa)
Rake angle = -10°Feed = 0.17 mm			
0.1	600	1600	700
0.3	1000	900	400
0.5	1300	2000	900
0.8	1400	2150	980
Rake angle = -10°Feed = 0.24 mm			
0.1	1150	1800	820
0.3	1350	2100	960
0.5	1450	2300	1000
0.8	1700	2600	1180
Rake angle = -25°Feed = 0.17 mm			
0.1	1000	1500	680
0.3	1200	850	780
0.5	1220	800	950
0.8	1300	2000	880
Rake angle = -25°Feed = 0.24 mm			
0.1	1200	1800	820
0.3	1220	1800	920
0.5	1250	1900	1000
0.8	1700	2000	1180
Rake angle = -40°Feed = 0.17 mm			
0.1	1000	1600	700
0.3	1550	2400	1100
0.5	1100	1500	800
0.8	1850	1800	820
Rake angle = -40°Feed = 0.24 mm			
0.1	2200	3400	810
0.3	2700	2800	920
0.5	2250	2750	1000
0.8	2600	4100	1190

Table 4: Distribution of mean stress along rake face in (MPa) for primary rake angle -10° and feed rate = 0.24

Landwidth (mm)/0.1	0.3	0.5	0.8
Position along rake face			
-662	-540	-559	-543
-577	-500	-494	-496
-424	-380	-397	-432
-154	-162	-172	-210
42	45	48	45
139	154	170	193
255	287	317	369
392	442	488	570
559	631	694	810
708	800	677	1024
1185	1340	1467	1170

Table 5: Distribution of mean stress along rake face in (MPa) for primary rake angle -25° and feed rate = 0.17mm/rev

Landwidth (mm)/0.1	0.3	0.5	0.8
Position along rake face			
-553	-516	-400	1283
-463	-434	-390	773
-330	-322	-310	616
-99	-119	-120	439
57	51	35	291
136	142	145	161
233	252	267	52
300	382	409	-135
500	539	578	-305
700	679	730	-368
1000	1131	1217	-435

Table 6: Distribution of mean stress along rake face in (MPa) for primary rake angle -25° and feed rate = 0.24 mm/rev

Landwidth (mm)/0.1	0.3	0.5	0.8
Position along rake face			
-663	-600	-500	-544
-563	-517	-450	-478
-407	-392	-400	-200
-134	-159	-200	39
56	43	-28	175
151	149	88	336
266	277	221	519
404	427	375	738
571	608	561	933
721	770	730	1558
1178	1290	1248	1700

Table 7: Distribution of average stress along rake face in (MPa) for primary rake angle -40° and feed rate = 0.17mm/rev

Landwidth (mm)/0.1	0.3	0.5	0.8
Position along rake face			
-566	-706	-503	-451
-485	-556	-420	-370
-329	-384	-323	-297
-98	-107	-137	-132
57	107	41	47
136	226	138	148
233	371	254	268
348	543	333	405
490	752	550	570
550	936	700	715
1021	1548	1160	1860

Von Mises stress: The relation of von Mises stress versus the distance along the rake face of the cutting edge is shown in Fig. 12 using the primary rake angle of -10°, it can be noticed that von Mises stress for land width 0.1 mm is high at the tip (1000 MPa) compression which is less than the yield stress of cutting inserts material (4000 MPa) by 75% when land width is 0.3 mm, the von Mises stress at the tip is 410 MPa which has a reduction of 59% compared with land width of 0.1 mm. When the feed is increased to 0.24 mm/rev Fig. 13,

Table 8: Distribution of average stress along rake face in (MPa) for primary rake angle -40°, and feed rate = 0.24 mm/rev

Landwidth (mm)/0.1	0.3	0.5	0.8
Position along rake face			
-1226	-1318	-1072	-1015
-1036	-1076	-955	-849
-743	-774	-781	-694
-242	-265	-394	-327
106	148	5.2	82
280	370	212	308
492	641	453	578
743	953	737	885
1050	1343	1375	1251
1323	1670	1900	1578
2210	2800	2330	2624

Table 9: Distribution of maximum shear stress

Position along rake face	Feed land width 0.1	0.3	0.5	0.8	0.1	0.3	0.5	0.8
	-10* and 0.17 mm/rev				**-10* and 0.24 mm/rev**			
1	480	206	408	356	550	501	482	436
2	373	256	339	294	483	422	390	376
3	267	203	292	274	348	343	340	364
4	117	59	166	177	158	167	196	245
5	66	41	81	98	68	79	91	114
6	136	81	168	195	147	167	187	220
7	232	137	291	329	259	280	326	383
8	351	206	444	494	400	452	500	580
9	489	286	618	681	582	635	700	816
10	681	307	862	940	790	890	975	1136
11	707	411	894	968	824	928	1013	1176
	-25* and 0.17 mm/rev				**-25* and 0.24 mm/rev**			
1	458	430	496	385	548	496	431	433
2	383	346	412	282	445	412	405	357
3	254	270	331	258	332	331	390	339
4	109	133	170	166	142	170	259	228
5	70	72	77	91	75	77	96	106
6	140	151	162	179	158	162	123	203
7	235	267	284	302	270	284	236	351
8	354	390	437	452	411	437	380	535
9	493	542	612	622	576	612	567	745
10	683	755	875	855	801	857	814	1033
11	702	783	983	880	826	893	880	1068
	-40* and 0.17 mm/rev				**-40* and 0.24 mm/rev**			
1	461	599	414	370	2139	1103	850	822
2	364	450	330	287	1752	860	731	648
3	253	314	279	251	1256	640	657	580
4	108	144	151	157	505	304	403	372
5	70	122	74	84	266	192	151	183
6	141	237	152	166	579	390	260	354
7	236	377	282	279	994	852	479	604
8	354	554	400	419	1508	979	762	915
9	491	770	555	575	2109	1352	1086	1256
10	683	1040	770	790	2800	1800	1200	1700
11	709	1100	800	830	3400	1937	1400	1800

the von Mises has the same trend but has a greater value becauseof high cutting load. From the above results and discussions, the optimum land width for these primary rake angles -10° was 0.3 mm which develops a minimum value of von Mises stress compared with other land widths. For rake angle -25° (Fig. 14), the von Mises stress, (0.1 mm land width) at the fixation point (1531 MPa). However, the results of the von Mises mean stress and maximum shear stress are shown in Table 1 for different rake angles with different feed and land widths.

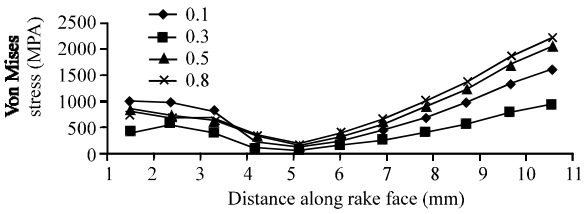

Fig. 12: Distribution of von Mises stress along rake face (primary angel -10, feed = 0.17 mm)

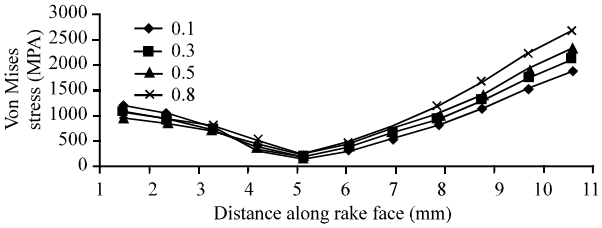

Fig. 13: Distribution of von Mises stress along rake face (primary angel -10, feed = 0.24 mm)

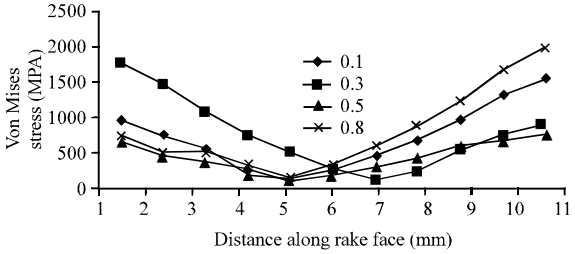

Fig. 14: Distribution of von Mises stress along rake face (primary angel -25, feed = 0.17 mm)

CONCLUSION

The concept of using double rake tooling has proved to be a good approach for better cutting tool performance and the resulting cutting loads change their direction so, as to put the tool under more favorable stress condition.

The optimum geometry was as follows: Primary rake (-10°), optimum land width 0.3 mm. Primary rake (-25°), optimum land width 0.5 mm. Primary rake (-40°), optimum land width 0.8 mm. The tensile region along the rake face is found to be beginning at approximately (1-1.5) times the contact length from the cutting edge.

REFERENCES

Ahmed, M.M., W.A. Draper and R.T. Derricott, 1989. An application of the FEM to the prediction of cutting tool performance. Intl. J. Mach. Tools Manuf., 29: 197-206.

Bagley, F.L., 1961. Turning hardened tool steel with ceramic tool. Tool Manuf. Eng., 46: 99-101.

Beer, F.P., E.R. Johnston Jr, J.T. DeWolf and D.F. Mazurek, 2014. Mechanics of Materials. 7th Edn., McGraw-Hill Education, New York, USA., ISBN:978-0073398235, Pages: 896.

Chandrasekaran, H. and R. Nagarajan, 1977. Influence of flank wear on the stresses in a cutting tool. J. Eng. Ind., 99: 566-577.

Draper, W.A. and G. Barrow, 1977. Double Rake Tooling-the Development of High Strength Tool Geometry. In: Manufacturing Engineering, Leicester Polytechnic, Stout, K.J., E.G. Pink and T.G. King (Eds.). School of Mechanical and Production Engineering, Leicester, England, pp: EQ1-EQ5.

Draper, W.A., 1974. An investigation into the optimum machining conditions of high strength steels. Ph.D Thesis, University of Manchester Institute of Science and Technology, Manchester, England.

Fowler, J.O., 1980. The cutting performance of coated carbide tools. Ph.D Thesis, Council for National Academic Awards, UK.

Sen, G.C. and A. Bhattacharyya, 1999. Principle of Metal Cutting. New Central Book Agency Private Limited, New Delhi, India,.

Venkatesh, V.C. and H. Chandrasekaran, 1982. Experimental Techniques in Metal Cutting. Prentice-Hall of India, New Delhi, India, ISBN:9780876920466, Pages: 525.

Vgural, A.C., 2009. Stresses in Beams, Plates and Shells. 3rd Edn., Taylor & Francis, Abingdon, UK., ISBN:9781439802700, Pages: 596.

Wadhwa, E.A.S., 2012. Engineering Material and Metallurgy. Laxmi Publications, India,.

Younis, M.A., 1992. Mechanical and thermal stresses in clamped, brazed and bonded carbide tools. J. Eng. Ind., 114: 377-385.

Zorev, N.N., 1963. Machining steel with a carbide tipped tool in interrupted heavy cutting conditions. Russ. Eng. J., 43: 43-46.